The electronic conductivity of Ca-Al metallic glasses

1990 J. Phys.: Condens. Matter 2 7287

(http://iopscience.iop.org/0953-8984/2/35/004)

J. Phys.: Condens. Matter **2** (1990) 7287–7302. Printed in the UK

The electronic conductivity of Ca–Al metallic glasses

B J Hickey†, S Lyon‡, G Bushnell-Wye‡, J Finney‡, M A Howson† and G J Morgan†

† Department of Physics, The University of Leeds, Leeds LS2 9JT, UK

‡ Birkbeck College, University of London, Malet Street, London WC1E 7HX, UK

Received 30 April 1990

Abstact. The magnitude and behaviour of the conductivity in Ca_xAl_{1-x} is of considerable interest as an example of a system with high resistivity where theories of weak and strong localisation can be tested without the complicating presence of transition metals and a corresponding high density of d states. In this paper we present computations of the density of states, the spectral function and the electrical resistivity using hard sphere structural models containing 216 atoms with periodic boundary conditions and pseudopotentials from a previous theoretical calculation. The computed resistivity follows quite well the general behaviour observed experimentally but it is rather larger and we show how this discrepancy can be accounted for by relatively small changes in the pseudopotential.

1. Introduction

In a recent paper (Howson *et al* 1988) we have investigated the role of quantum interference effects in enhancing the electrical resistivity of Ca_xAl_{1-x} amorphous metals over that which would be obtained using the Faber–Ziman (1965) theory of simple amorphous or liquid metal alloys. Although these alloys are 'simple' in comparison with transition metal alloys the calculation of the resistivity of Ca, Ba, or Sr using pseudopotentials is notoriously sensitive to the details of the pseudopotential (Moriarty 1972). This is because the Fermi energy is on the edge of the almost unoccupied d bands and $2K_F$ is close to the first peak in the structure factor $a(q)$ where K_F is the Fermi wavevector. In the paper by Howson *et al* the effects of quantum interference were assessed using the *simplest* treatment of general transport equations formulated by Morgan *et al* (1985) in which the density of states and spectral function are presumed not to be changed drastically from the free electron form. This was justified by appealing to numerical calculations of the densities of states and experimental specific heat data. The calculations used Percus–Yevick hard sphere structure factors (see Ashcroft and Langreth 1967) and pseudopotentials adjusted to give the same resistivity as pure liquid Al and Ca. The whole point of that work was to demonstrate the importance of quantum interference effects in enhancing the Faber–Ziman theory rather than pretending we can carry out an *ab initio* calculation which would give 'spot-on' answers with structure factors, and pseudopotentials obtained from first principles.

The purpose of our present paper is to take the *same* pseudopotentials together with *model* hard sphere structure factors and compute the electronic properties thus enabling us to assess our previous theoretical treatments as well as enabling us to test the numerical

0953-8984/90/357287 + 16 $03.50

method on a system for which we have experimental data. The numerical method is essentially that invented by Weaire and Williams (1977) adapted for a plane wave basis and we have already used this method to investigate the electronic properties of amorphous Si as a test case (Hickey and Morgan 1986, Morgan *et al* 1989, Burr and Morgan 1990) where excellent structural models are available and rather reliable pseudopotentials are at hand. It is to be emphasised that our intent is to understand the physics of these kinds of materials using well defined structural models and pseudopotentials rather than more refined forms which will no doubt be important in a completely quantitative theory. It is our belief that there are broader issues which are more important at this point in time.

In section 2 we describe the hard sphere structural models using algorithms described by Finney (1976) and make a comparison with the pair distribution functions obtained using the Percus–Yevick approximation and with molecular dynamics calculations performed by Hafner *et al* (1987). Section 2 is also concerned with the details of the pseudopotentials used for the alloy systems, while section 3 describes the calculations and results of the electronic transport properties using the equation of motion method in k-space, and we discuss the reasons why the computed resistivities turn out larger than the experimental and theoretical values obtained previously. The behaviour of the spectral functions are described in section 4.

2. The pseudopotentials and structural models

Our theoretical calculations for the Ca–Al system emplyed Percus–Yevick hard sphere structure factors as described in detail by Ashcroft and Langreth. The pseudopotential assumed for Al is the simple form

$$v(q) = 4\pi Ze^2[\cos(qR_0)/(q^2 + K_s^2)]$$

where K_s is the inverse Fermi–Thomas length calculated using free electron densities of states and R_0 is a fitting parameter to give the resistivity of *liquid* Al ($\rho = 24\ \mu\Omega$ cm), namely, $R_0 = 1.15$ au. The pseudopotential for Ca corresponds to that tabulated by Moriarty screened using the Fermi–Thomas approximation and scaled by a factor $(E_F^{Ca} - E_d^{Ca})/(E_F - E_d)$ where E_F^{Ca} is the Fermi energy of pure Ca, E_d^{Ca} is the position of the d band for pure Ca. E_F and E_d are the same parameters for the alloys system and $E_F - E_d$ was used to fit the experimental data *including* the effects of quantum interference corresponding to the *simplest* treatment of the Morgan *et al* equations. This scaling was only applied for values of q greater than $1.3K_F$ where K_F is the free electron wave vector for pure Ca as this is the part of the pseudopotential most important in describing scattering into the tail of the d states and the pseudopotential goes through zero at $1.3K_F$. We again emphasise that the point of this calculation was to demonstrate the importance of quantum interference in these alloys. However, we can now take these self-same potentials and specific hard model structures and perform numerical calculations using a plane wave representation and evaluate the conductivity using the equation of motion method in k-space (Hickey and Morgan 1986) and the method of Weaire and Williams for evaluating the Kubo–Greenwood formula (Kubo 1956, Greenwood 1958). Before describing these calculations in section 3, it is first necessary to discuss the model structures in relationship to the Percus–Yevick structures and the forms obtained from molecular dynamics using more realistic interatomic potentials (Hafner *et al* 1987).

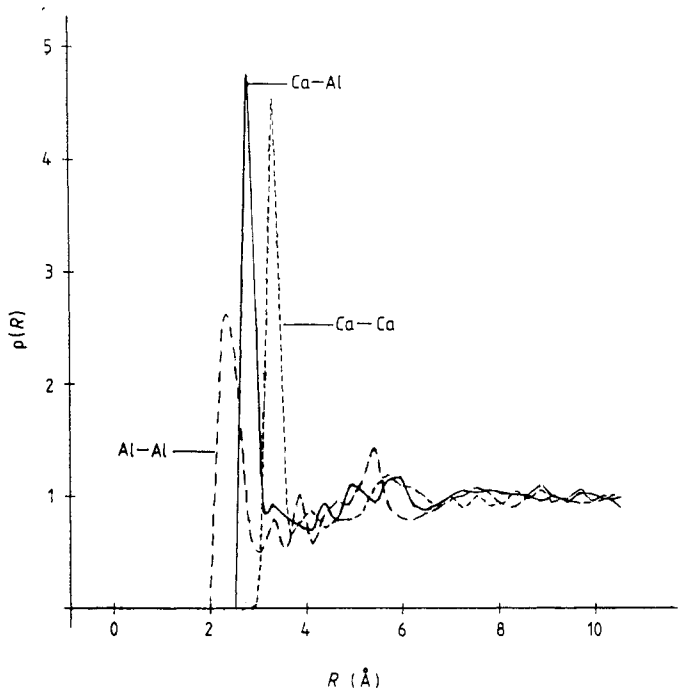

Figure 1. The partial pair distribution functions for $Ca_{0.6}Al_{0.4}$ obtained from the model structure.

The structural models and the Percus–Yevick structures were worked out using hard sphere radii corresponding to half the nearest-neighbour distances in crystalline Al and Ca divided by a 'softening' factor of 1.2 which yields hard sphere radii of 2.28 au for Al and 3.11 au for Ca. The packing fraction for Ca was chosen to be 0.43† and we then *enhanced* the Moriarty pseudopotential by a factor of 1.4 for $q > 1.3$ to give the right resistivity for *liquid* Ca ($\rho = 33\ \mu\Omega$ cm). This is reasonable as $(E_F^{Ca} - E_d^{Ca})$ is essentially a parameter in the theory. Glassy alloys of Ca_xAl_{1-x} have actually only been made for $0.5 < x < 0.8$ so we use the liquid state values for pure Ca and Al to extend the range of experimental values. Quantum interference effects are very small for the resistivities of pure liquid Ca and Al so this is also a sensible procedure. The densities of the alloys were taken from a linear interpolation between the densities of *crystalline* Ca (1530 kg m^{-3}) and Al (2700 kg m^{-3}) which agrees with experimental measurements to within five per cent. The calculations of the structure were performed for $0 < x < 1$ in steps of 0.2, and the packing fractions ζ_x are $\zeta_1 = 0.43$, $\zeta_{0.8} = 0.46$, $\zeta_{0.6} = 0.49$, $\zeta_{0.4} = 0.49$, $\zeta_{0.2} = 0.47$ and $\zeta_0 = 0.43$.

The method for generating the hard sphere structures has been described in detail by Finney (1983) and corresponds to relaxing from an initial random structure by repeated small displacements of the atoms until no two spheres overlap. The resulting structures are also constrained to be periodic and each structure contains 216 atoms in total within a box having sides of length L determined by the density. The partial pair distribution functions have been obtained using 'bins' of width of 0.25 Å. Every atom in the structure is used in the averaging progress because of the periodic boundary conditions.

† Note that in the paper by Howson, Hickey and Morgan the packing fraction for Ca was misquoted as 0.483.

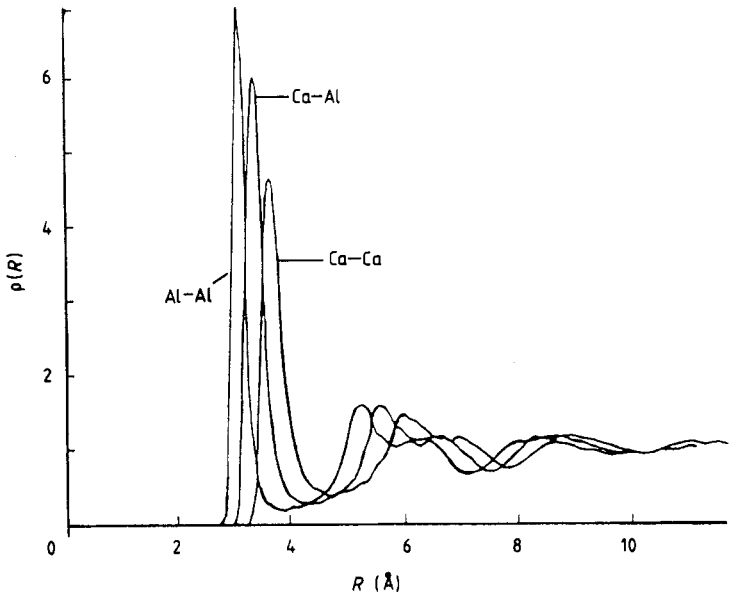

Figure 2. The partial pair distribution functions for $Ca_{0.6}Al_{0.4}$ obtained from molecular dynamics computations by Hafner *et al* (1987).

In figures 1 and 2 we show the partial pair distribution functions for $x = 0.6$ and compare the behaviour with that obtained by Hafner *et al* using molecular dynamics for the liquid state followed by rapid quenching of the structure. There are clear differences: the most obvious being the relative and maximum heights of the first peak in the calcium

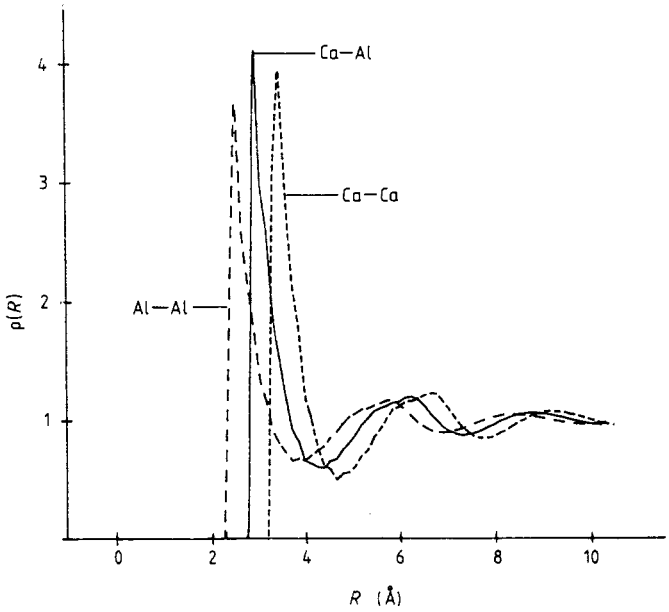

Figure 3. The partial pair distribution functions for $Ca_{0.6}Al_{0.4}$ obtained from the Percus–Yevick hard sphere theory.

calcium distribution (P_{CaCa}) and the Al–Al distributions (P_{AlAl}). The height of the P_{AlCa} first peak is higher than the other two for our model, whereas the molecular dynamics calculation gives a peak height which is intermediate between the other two. This is probably due to the fact that the interatomic potentials used by Hafner *et al* have minima near the peak position and the depth of the minimum is greatest for Al–Al interactions and weakest for Ca–Ca interactions. From the point of view of this paper, however, it is more relevant to compare the model distributions with those of the Percus–Yevick theory obtained by inverting the partial structure factors using numerical integration. These are shown in figure 3 and we now see a better correspondence between the behaviour of the peak heights for the model and the theory. The behaviour of the pair distributions for pure Al and Ca is shown in figures 4–7, and it can be seen that there is again a reasonable degree of similarity between the model and theory. Although the

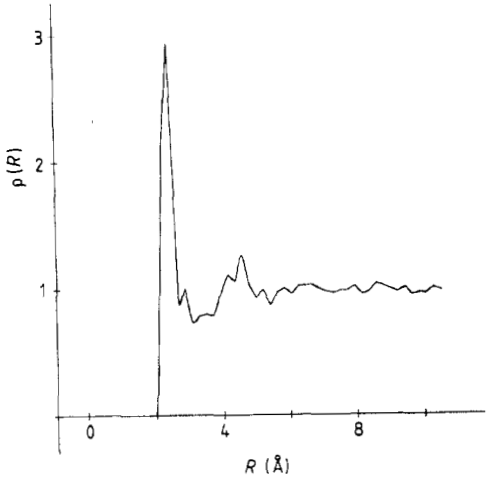

Figure 4. The model pair distribution for Al.

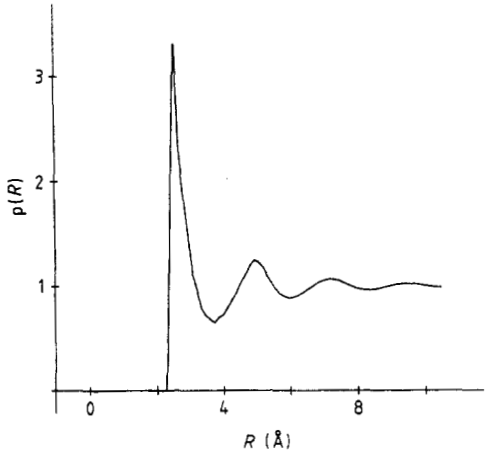

Figure 5. The Percus–Yevick distribution for Al.

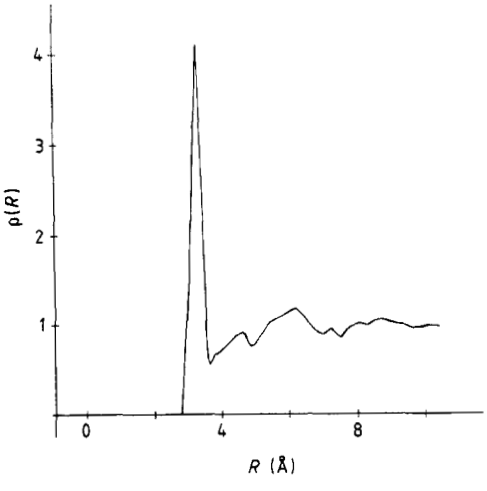

Figure 6. The model pair distribution for Ca.

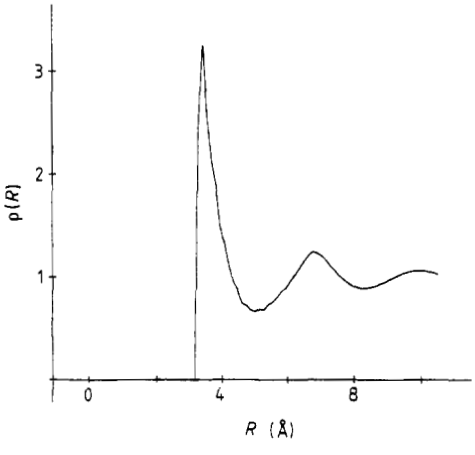

Figure 7. The Percus–Yevick pair distribution for Ca.

model structures are not completely ideal for making a precise comparison with the calculations of Howson *et al*, this is not of overriding importance since our main concern is to carry out computations which demonstrate how very large resistivities arise in this kind of system without the necessity for a low density of states and to show that the method can be used successfully on realistic models to compute a range of electronic properties. As far as we are aware this is the first calculation of this kind.

3. The computation of the electronic transport properties

The equation of motion method in $\boldsymbol{K}$-space has been used previously to compute the electronic structure of amorphous Si using a fully bonded model containing 216 atoms and about fourteen plane waves per atom (Hickey and Morgan 1986.) It has also been used to compute the self-energy, the conductivity and the diffusion coefficient in the region of the energy gap which is an extremely demanding task and we showed the probable position of mobility edges (Hickey *et al* 1989). The application of the method to metals is less demanding because we are not trying to resolve fine details in the behaviour of the conductivity and we only need the conductivity at the Fermi energy. We again use about fourteen plane waves per atom, and the calculation proceeds as described by Hickey and Morgan (1986) and Hickey *et al* (1989).

The wave function is written as

$$\psi(\boldsymbol{r}t) = \Omega^{-1/2} \sum_{\boldsymbol{K}}^{K_C} a_{\boldsymbol{K}}(t) \exp(\mathrm{i}\boldsymbol{K}\cdot\boldsymbol{r}) \tag{1}$$

where $K_C = 1.92\,K_F$ and we then solve for the amplitudes as a function of time (Alben *et al* 1975) using the simplest leap-frog method (Mackinnon 1984). The density of states $g(E)$, the Green function $G_{\boldsymbol{K}\boldsymbol{K}}(E)$, the self-energy $\Gamma(\boldsymbol{K}E)$ and the spectral function $\rho(\boldsymbol{K}E)$ can then be obtained by using various initial conditions for the amplitudes $a_{\boldsymbol{K}}$. The conductivity has been calculated in the manner described by Weaire and Williams (1977), namely the conductivity as a function of energy is given by

$$\sigma_F(E) = \frac{2\pi e^2}{m^2\Omega} \sum_{\boldsymbol{K}} \sum_{\boldsymbol{K}'} K_x K'_x (\overline{a^*_{\boldsymbol{K}} a_{\boldsymbol{K}} a^*_{\boldsymbol{K}'} a_{\boldsymbol{K}'}} - \overline{a^*_{\boldsymbol{K}} a_{\boldsymbol{K}}}\;\overline{a^*_{\boldsymbol{K}'} a_{\boldsymbol{K}'}}) \tag{2}$$

where Ω is the volume of the system, the bars denote averages over time and σ_F denotes that the amplitudes $a_{\boldsymbol{K}}$ have been 'filtered' to retain eigenstates near to the required energy E. The filtering process is that described by Hickey *et al* (1985) whereby the amplitudes are chosen to have a random phase at $t = 0$, the amplitudes are calculated up to a time T_F and then filtered by integrating with

$$\pi^{-1} \sin(E_{\max} t/\hbar) \exp(\mathrm{i}Et/\hbar) t^{-1}.\dagger$$

$E_{\max}$ is the half width of the filter function which selects states near to the energy E. The form of this filter function has been shown in the paper by Hickey *et al* (1989). The half-width of this filtering function has been chosen to be 0.2 eV. The filtered amplitudes are then calculated as a function of time in order to construct the time averages required in equation (2). Some typical examples of the behaviour of $\sigma_F(E)$ (atomic units) as a function of the length of the time averaging are shown in figures 8 and 9 and it can be

† The factor of t^{-1} in this expression was omitted in Hickey *et al* (1990).

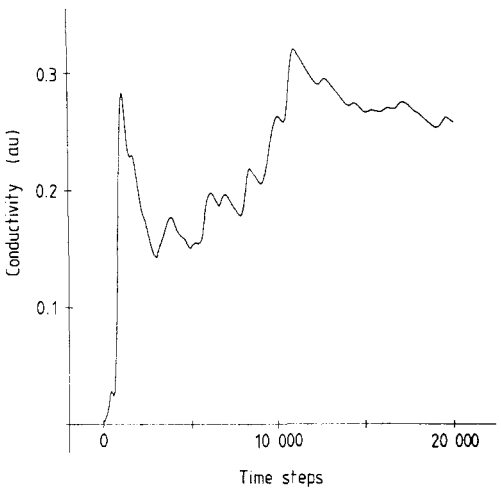

Figure 8. Typical behaviour of the conductivity σ_F in Ca as a function of the time of averaging. We use the average over the last 2500 time steps to calculate the conductivity in all cases.

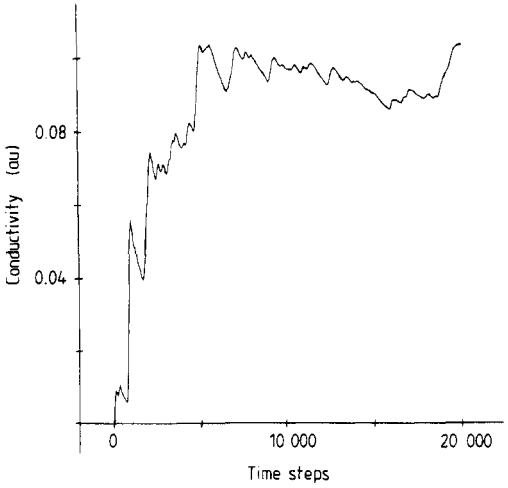

Figure 9. Typical behaviour of σ_F in $Ca_{0.6}Al_{0.4}$ as a function of time.

seen that the averages have settled down to values which are fluctuating by about $\pm 10\%$. Before discussing the details of the conductivity it is important to consider the density of states obtained for these alloys usiing the method described for a-Si (Hickey and Morgan 1986).

The method results in a density of states convoluted with a Lorentzian and our value of the half-width has been chosen to be 0.4 eV. In a-Si we deconvoluted the density of states to obtain the behaviour near the gap but this is not an important issue in the present context. However, the results in figure 10 have been deconvoluted using the iterative method (Hickey and Morgan 1986) but using *only* a single iteration so that we do make the density of states too spiky. The zero of energy is the Fermi energy which has been calculated by integrating the density of states and this is the reason for partially deconvoluting the density of states. The important thing to notice is that there are fluctuations due to the finite size of the system as the allowed values of $\boldsymbol{K}$ tend to cluster around particular values. The conductivity in the vicinity of the Fermi energy naturally fluctuates in a similar way, so that we average the value at E_F with four other values on either side of E_F in steps of 0.2 eV, which is the scale required to smooth out the fluctuations in the density of states. The behaviour of the conductivity correlates quite well with the density of states in some cases, as is shown in figure 11 for pure Al, but not in general, as is shown in figure 12 for Ca. It must be remembered that there will be real energy dependence of the conductivity superimposed on the fluctuations produced by the finite sizes of the system. In the case of Al the conductivity is a slowly varying function when calculated from the Morgan *et al* or Faber–Ziman theory. In Ca, however, the calculated variation with energy is very large, as indicated by a large calculated thermopower (Howson *et al* 1988).

The results of our computations for the resistivity are shown in figure 12 as a function of composition. Also shown are the experimental results, the fitted calculations of Howson *et al* including quantum interference effects and the results obtained from the Faber–Ziman theory. Clearly our computed resistivities are greater than the exper-

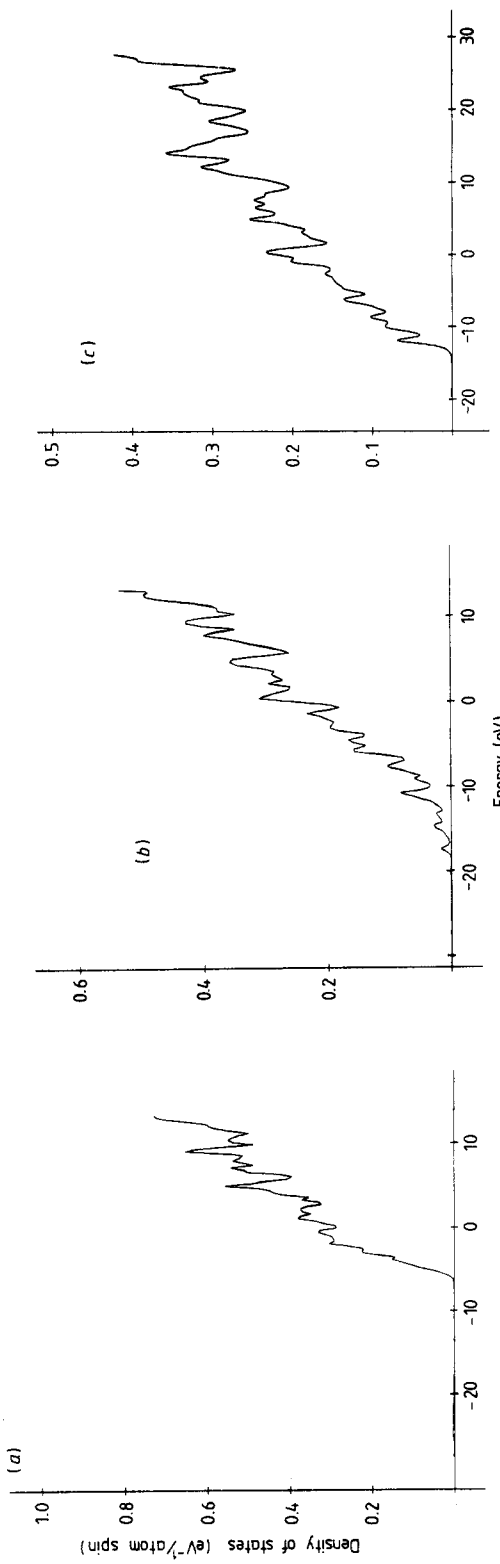

Figure 10. The density of states for Ca (*a*), $Ca_{0.6}Al_{0.4}$ (*b*) and Al (*c*). The zero is the value of the Fermi energy.

imental values, but the general behaviour as a function of composition is reproduced. Let us first consider the case of Al where the computed resistivity is 43 $\mu\Omega$ cm compared with an experimental value of 24 $\mu\Omega$ cm. This is actually an extremely reasonable result when one realises the very sensitive nature of the resistivity to pseudopotentials *and* structure factors. We have recalculated the resistivity for another computer generated model using the same parameters and obtain $\rho \simeq 50\ \mu\Omega$ cm which is in fair agreement. The pair distributions for our hard sphere results and the Percus–Yevick models are not in exact correspondence so the difference in the resistivities is not of major concern. The much larger computed resistivity of Ca ($198 \pm 60\ \mu\Omega$ cm) is of much greater importance and interest and an explanation of this is also relevant to understanding the generally larger resistivities across the composition range.

The calculations of the resistivity by Howson *et al* (1988), which are shown in figure 13, were obtained using the simplest form of the equations derived by Morgan *et al* (1988) which ignored deviations from a free electron-like density of states and the effects of lifetime broadening on the elastic scattering rate. The parameters of the pseudopotentials and structure factors were then deduced by fitting the measured resistivities and, as explained before, to achieve this we enhanced the pseudopotential tabulated by Moriarty by a factor of 1.4 for $q > 1.3\ K_F$ because the tabulated pseudopotential gives a resistivity of 17.5 $\mu\Omega$ cm. This does not lead to a discontinuity in the pseudopotential as it goes through zero at $q = 1.3\ K_F$. Accordingly, we have repeated

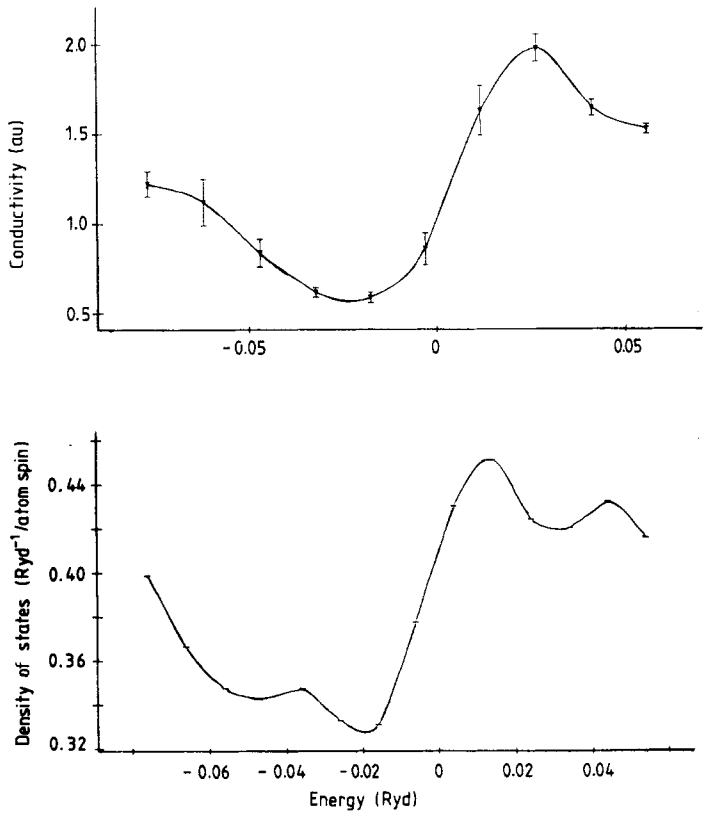

Figure 11. The behaviour of the conductivity (upper diagram) and density of states for Al in the neighbourhood of the Fermi energy which is the energy zero in these diagrams.

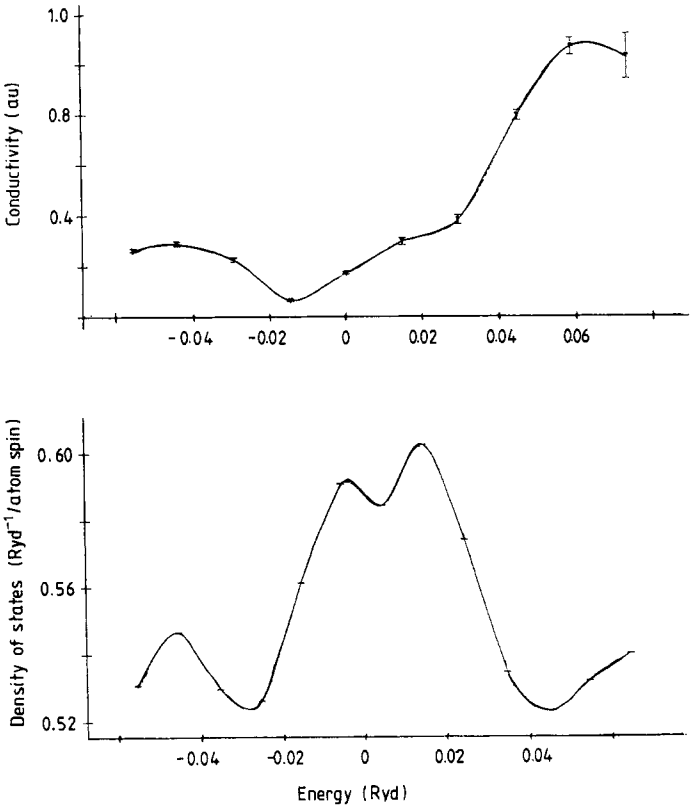

Figure 12. The behaviour of the conductivity (upper diagram) and density of states for Ca. Again the zero corresponds to the Fermi energy.

the computer simulation for Ca using the pseudopotential unenhanced by a factor of 1.4 and we obtain the result $\rho = 28 \pm 5\ \mu\Omega$ cm. If the Faber–Ziman theory were precise for this pseudopotential the maximum change in the resistivity would be a reduction of a factor of two but we see a reduction in the resistivity by about an order of magnitude, indicating that for the *enhanced* potential the simple Faber–Ziman theory is not valid. Clearly the resistivity is especially sensitive to the behaviour of the pseudopotential and we now discuss this sensitivity in relationship to the Morganc *et al* theory (Morgan *et al* 1985).

$$\sum_{K'} T(\boldsymbol{K}\boldsymbol{K}')(\bar{\rho}'(\boldsymbol{K}) - \bar{\rho}'(\boldsymbol{K}')) = -e\boldsymbol{\varepsilon} \cdot \frac{\hbar \boldsymbol{K}}{m} \rho(KE_F)(1 + \gamma(K)) \tag{3}$$

where we have assumed, as is the case, that the lifetime broadening is much greater than kT. In (3) $\bar{\rho}'$ denotes the deviation from equilibrium, $\rho(KE_F)$ is the spectral function at the Fermi energy and $\gamma(K)$ is a function which cuts off the rather long-range tail of ρ which can lead to unphysical divergences. $T(\boldsymbol{K}\boldsymbol{K}')$ is a generalised scattering kernel, analogous to the vertex part in the Bethe–Salpeter equation (see, for example, Vollhardt and Wölfle 1980) and includes weak and strong localisation effects in general. In the case of Ca, which has a fairly low resistivity, we are primarily interested in the part of T,

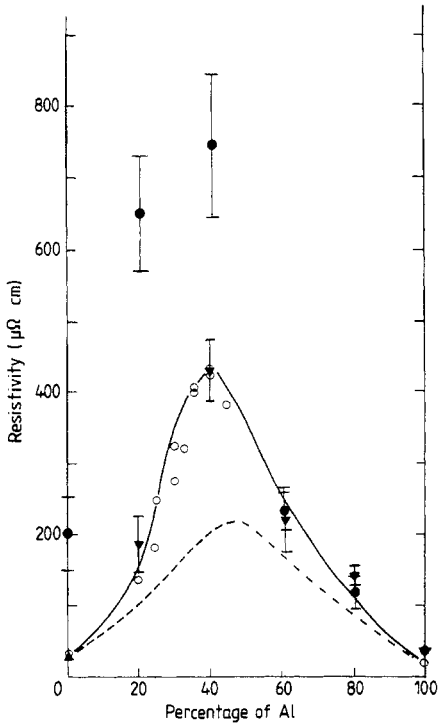

Figure 13. The resistivity as a function of the percentage of Al. The full circles denote the computed values for the enhanced pseudopotential while the full curve corresponds to a simplified form of the Morgan *et al* theory for the same pseudopotentials. The broken curve corresponds to the Faber–Ziman theory. The open circles correspond to the experimental values though those for pure Ca and Al are liquid state values. The full triangles coresond to computed values for the unenhanced forms of the Moriarty pseudopotential and good agreement is obtained with experiment.

termed T_1 by Morgan *et al* (1985) which does not contain quantum interference effects, namely

$$T_1(\boldsymbol{K}\boldsymbol{K}') \simeq \frac{2\pi}{\hbar}\frac{N}{\Omega^2}\frac{v^2(\boldsymbol{K}-\boldsymbol{K}')a(\boldsymbol{K}-\boldsymbol{K}')\hbar\tau^{-1}(\boldsymbol{K}+\boldsymbol{K}')/2}{\pi\{[(\hbar^2/2m)(K^2-K'^2)]^2+[\hbar\tau^{-1}(\boldsymbol{K}+\boldsymbol{K}')/2]^2\}} \tag{4}$$

where N/Ω is the number of atoms/unit volume, $a(q)$ is the structure factor and

$$\tau^{-1}(K) = \sum_{K'} T_1(\boldsymbol{K}\boldsymbol{K}'). \tag{5}$$

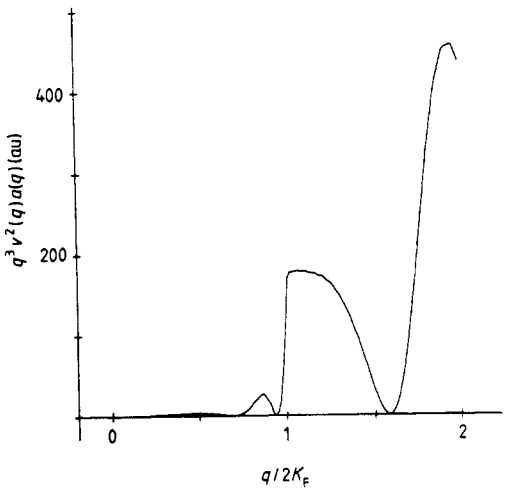

Figure 14. The behaviour of $q^3v^2(q)a(q)$ for Ca showing the very sharp rise for values of $q > 2K_F$.

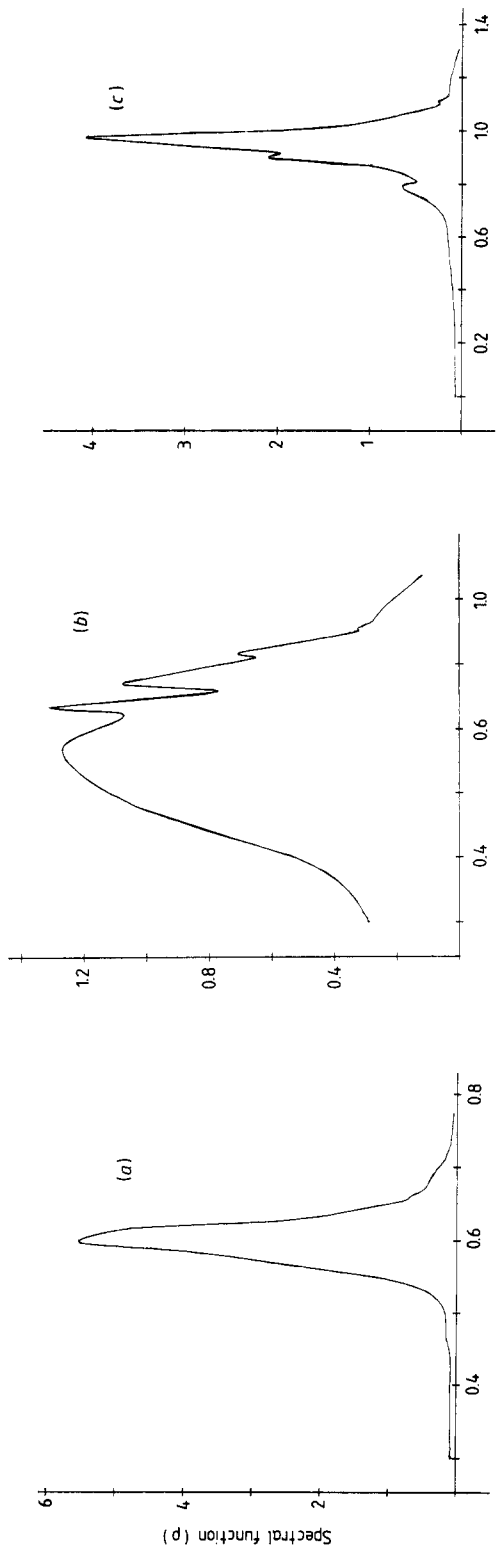

Figure 15. The behaviour of the spectral function (ρ) at the Fermi energy as a function of K for (*a*) Ca, (*b*) $Ca_{0.6}Al_{0.4}$ and (*c*) Al.

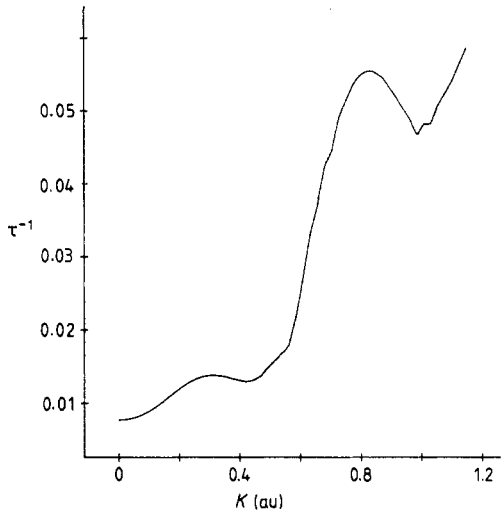

Figure 16. A self-consistent solution of equation (5) yielding τ^{-1} as a function of K.

In the Faber–Ziman theory, the Lorentzian-like part in (4) would be replaced by a Dirac delta function, and $\rho(1 + \gamma)$ in (3) would be replaced by the derivative of the Fermi function. Perhaps the general point should be made that, for liquid and amorphous metals life time broadening of states is always much greater than kT. The reason why the replacement of the Fermi function by $\rho(1 + \gamma)$ is usually not of major importance is that if $\rho(1 + \gamma)$ is reasonably narrow and free electron like, and occurs in integrals which are slowly varying as a function of K then $\rho(1 + \gamma)$ can be treated essentially as a delta function.

In figure 14 we show the behaviour of $q^3v^2(q)a(q)$ where $v(q)$ is the pseudopotential and $a(q)$ is the structure factor used in fitting the resistivity of Ca. This is the argument of the integral which determines τ_{FZ}^{-1}, the transport lifetime in the Faber–Ziman theory (see Morgan *et al* 1988). The plot is in units of $2K_F$ so $q = 1$ is the maximum value of q in the integral

$$\tau_{FZ}^{-1} = \frac{m}{2\pi\hbar^3}\frac{n}{K_F^3}\int_0^{2K_F} \mathrm{d}q\, q^3v^2(q)a(q) \tag{6}$$

where n is the number of atoms/unit volume. The important point is that q^3v^2a rises *extremely* rapidly for $q > 2K_F$ so that the lifetime broadening present in $\rho(K)$ and (4) will enable the large parts of this function to be sampled. Lifetime broadening has a double effect which will enhance the resistivity. In figure 15(a) we show the computed spectral function at E_F as a function of K for the *enhanced* pseudopotential and it can be seen that the full width is about 1 eV which should be compared with a Fermi energy of about 5 eV. In figure 15 we show a self-consistent calculation of τ^{-1} as defined by equation (5). The behaviour of $\tau^{-1}((\boldsymbol{K} + \boldsymbol{K}')/2)$ is such that it would be zero for $\boldsymbol{K} = -\boldsymbol{K}'$ if calculated non-self-consistently reducing the effect of broadening for scattering into the backward direction. However, if the resistivity of 'amorphous' Ca is calculated without quantum interference effects using the self-consistent values shown in figure 16, we obtain a resistivity of 57 $\mu\Omega$ cm which is about double that obtained from the Faber–Ziman theory. It can be seen, therefore, that lifetime broadening effects can have a strong effect on the resistivity which will then be further enhanced by quantum

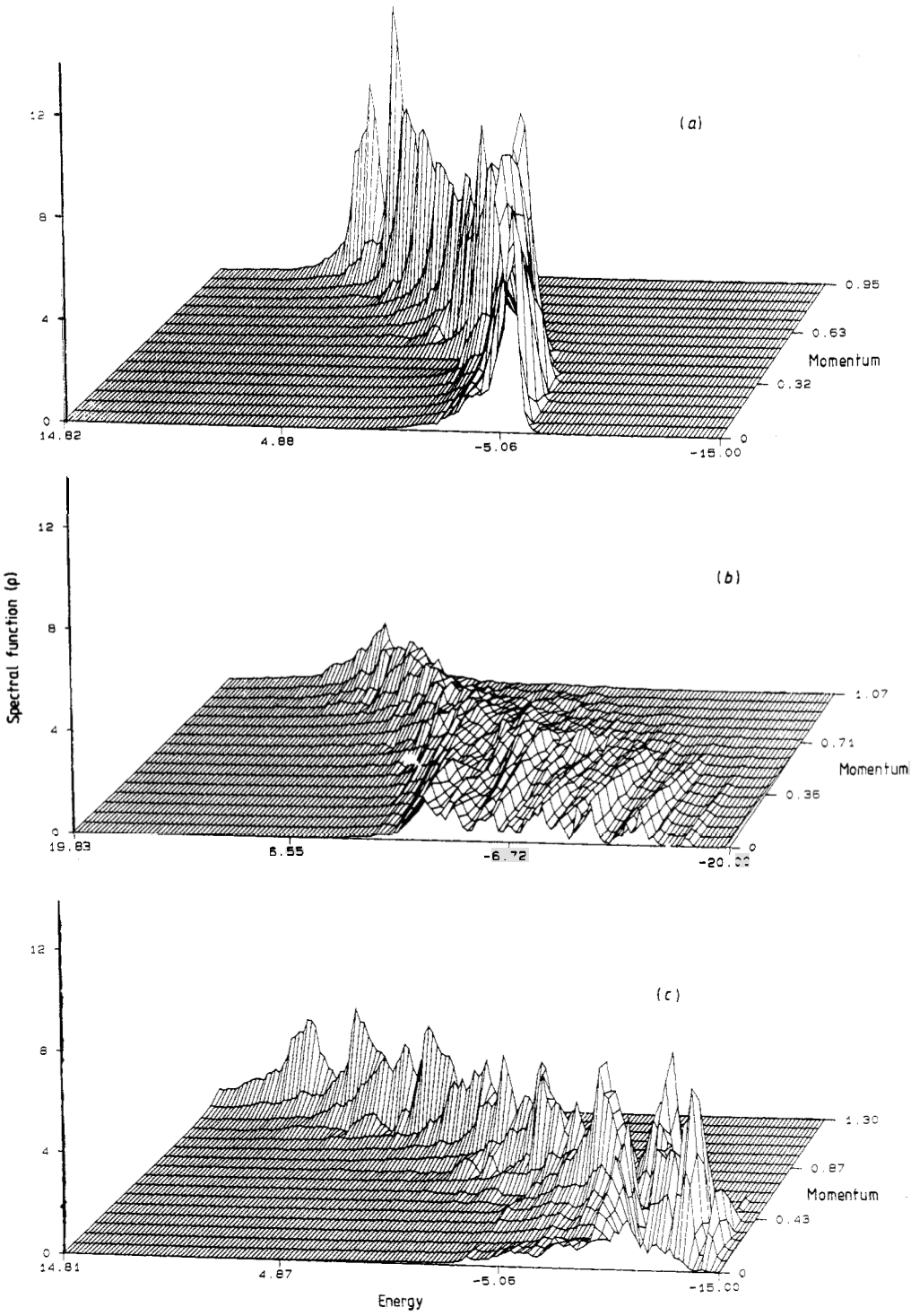

Figure 17. The spectral function (ρ) as a function of E and K (in au) with the Fermi energy as the energy zero. (*a*) Ca, (*b*) $Ca_{0.6}Al_{0.4}$, (*c*) Al.

interference. These facts qualitatively illustrate how a fairly moderate enhancement of the pseudopotential can result in a large increase in the resistivities which was not appreciated when we embarked on the computations described here.

We have repeated the calculations of the resistivity right across the composition range using the pseudopotential unenhanced by a factor of 1.4. The results now agree extremely well with the experimental values and provide a basis for the investigation of properties such as the magnetoresistivity. We now turn to behaviour of the spectral functions calculated using the enhanced pseudopotentials.

4. The spectral functions

The spectral function can be calculated using the initial condition $a_{\boldsymbol{K}}(0) = \delta_{\boldsymbol{K}\boldsymbol{K}_0}$. If we denote the amplitude of the $\boldsymbol{K}$ states at later times by $G_{\boldsymbol{K}\boldsymbol{K}_0}$ then the Fourier transform (atomic units)

$$G^{\mathrm{c}}_{\boldsymbol{K}\boldsymbol{K}_0}(E) = \int_0^{T_{\max}} \exp(-\varepsilon t) G_{\boldsymbol{K}\boldsymbol{K}_0}(t) \exp(\mathrm{i}Et/\hbar)\, \mathrm{d}t \tag{7}$$

yields the Green function $G_{\boldsymbol{K}\boldsymbol{K}_0}$ convoluted with a Lorentzian of half width ε. The magnitude of ε is chosen so that the value of the integrand is negligible at $T_{\max}$ which is the run time over which the amplitudes are allowed to evolve. For large systems we may write

$$G_{\boldsymbol{K}\boldsymbol{K}}(E) = (E - K^2 - \Gamma(KE))^{-1} \tag{8}$$

which corresponds to equating the ensemble average of the Green function to the diagonal component of G for a particular large system. If we define a self-energy for our small system in this way, then of course the self-energy so obtained will be dependent on the precise details of the model but, as shown in our calculations for amorphous Si, the behaviour of Γ so defined is very informative and the general behaviour is representative of a large system though of course the fine detail will depend on the details of the model structures. The real part of Γ (Γ_{R}) and the imaginary part of Γ (Γ_{I}) can be obtained from the calculated real and imaginary parts of G. The spectral function defined by

$$\rho(KE) = (1/\pi)\, \Gamma_{\mathrm{I}}/[(E - K^2 - \Gamma_{\mathrm{R}})^2 + \Gamma_{\mathrm{I}}^2] \tag{9}$$

may then be obtained either by calculating Γ_{R} and Γ_{I} separately or from the imaginary part of $G_{\boldsymbol{K}\boldsymbol{K}}$. Our procedure is to first partly deconvolute $G_{\boldsymbol{K}\boldsymbol{K}}(E)$ using an iterative method (Hickey and Morgan 1986) then calculate Γ_{R} or Γ_{I}. The reason for only partly deconvoluting (by a single iteration) is that we do not wish to completely deconvolute the density of states into a set of delta-function-like peaks, yet we want to remove the smoothing effect of the finite run time $T_{\max}$. In figures 15(*a*), (*b*) and (*c*) we show the form of the spectral function at E_{F} as a function of K for Ca, $Ca_{0.6}Al_{0.4}$ and Al. The relative sharpness of the peaks for pure Ca and Al is to be expected but the *very* broad nature of the spectral function for $Ca_{0.6}Al_{0.4}$ was rather unexpected despite the large resistivity. It can be seen that the assumption of a reasonably well defined peak is likely to be inappropriate in this case despite the fairly free electron-like density of states.

In figures 17(*a*), (*b*) and (*c*) we show representative plots of the spectral functions for the same alloys. The nearly free-electron-like form is apparent for Ca and Al over most of the energy range but the drastic broadening is apparent for $Ca_{0.6}Al_{0.4}$, especially

at the bottom of the band. The broadening will be reduced for the unenhanced pseudopotential for Ca but the same kind of structure is to be expected for the weaker pseudopotential.

5. Conclusions

The calculations reported here demonstrate a number of important points, not least of which is that one can perform numerical calculations for small systems described by a pseudopotential, and obtain sensible results.

We have also shown that very large resistivities may be obtained without a low density of states in a metallic system, hence raising the possibility of obtaining an Anderson transition with a high density of electronic states as we have sought to do by making alloys of CaAl with Ba (Howson *et al* 1988).

The theoretical calculations of Howson *et al* (1988) represented a simple treatment of the Morgan *et al* (1985) theory of localisation where the effect of lifetime broadening was ignored and we placed our emphasis on illustrating the importance of quantum interference effects. The calculations in this paper show that broadening of the spectral function can be very large in the middle of the concentration range and that broadening can considerably enhance the resistivity for elements like Ca, when described by a generalised pseudopotential.

Finally, this paper paves the way for carrying out calculations using a hybrid scheme of plane waves and localised d orbitals to discuss amorphous transition metal alloys, where a very important objective would be to calculate the Hall coefficient along the lines described here.

References

Alben R, Blume M, Krakauer H and Schwartz L 1975 *Phys. Rev.* B **12** 4090
Ashcroft N W and Langreth D C 1967 *Phys. Rev.* B **159** 500
Faber T E and Ziman J M 1965 *Phil. Mag.* **11** 153
Finney J L 1976 *Mater. Sci. Eng.* **23** 199
Greenwood D A 1958 *Proc. Phys. Soc.* **71** 585
Hafner J, Egami T, Aur S and Giessen B C 1987 *J. Phys. F: Met. Phys.* **17** 1807
Hickey B J, Burr J N and Morgan G J 1990 *Phil. Mag. Lett.* **61** 161
Hickey B J and Morgan G J 1986 *J. Phys. C: Solid State Phys.* **19** 6195
Howson M A, Hickey B J and Morgan G J 1988 *Phys. Rev.* B **38** 5267
Kubo R 1956 *Can. J. Phys.* **34** 1274
MacKinnon A 1984 *The Recursion Method and its Applications* ed D Pettifor and D L Weaire (Berlin: Springer)
Morgan G J, Hickey B J and Burr J N 1989 *J. Non-Cryst. Solids* **114** 262
Morgan G J, Howson M A and Šaub K 1985 *J. Phys. F: Met. Phys.* **15** 2157
Moriarty J A 1972 *Phys. Rev.* B **6** 445
Vollhardt D and Wölfle P 1980 *Phys. Rev.* B **22** 4666
Weaire D L and Williams A R 1977 *J. Phys. C: Solid State Phys.* **10** 1239